Plant, Cell & Environment

Plant, Cell and Environment (2012) **35**, 1647–1662 doi: 10.1111/j.1365-3040.2012.02515.x

Simple models for stomatal conductance derived from a process model: cross-validation against sap flux data

THOMAS N. BUCKLEY[1,3], TARRYN L. TURNBULL[2,3] & MARK A. ADAMS[2,3]

[1]Department of Biology, Sonoma State University, 1801 E Cotati Ave, Rohnert Park, CA 94928, USA, [2]Faculty of Agriculture and Environment, University of Sydney, Sydney, New South Wales, Australia and [3]Bushfire Cooperative Research Centre, Melbourne, Victoria, Australia

ABSTRACT

Representation of stomatal physiology in models of plant-atmosphere gas exchange is minimal, and direct application of process-based models is limited by difficulty of parameter estimation. We derived simple models of stomatal conductance from a recent process-based model, and cross-validated them against measurements of sap flux (176–365 d in length) in 36 individual trees of two age classes for two *Eucalyptus* species across seven sites in the mountains of southeastern Australia. The derived models – which are driven by irradiance and evaporative demand and have two to four parameters that represent sums and products of biophysical parameters in the process model – reproduced a median 83–89% of observed variance in half-hourly and diurnally averaged sap flux, and performed similarly whether fitted using a random sample of all data or using 1 month of data from spring or autumn. Our simple models are an advance in predicting plant water use because their parameters are transparently related to reduced processes and properties, enabling easy accommodation of improved knowledge about how those parameters respond to environmental change and differ among species.

Key-words: Eucalyptus; stomatal conductance model; transpiration.

INTRODUCTION

Transpiration by trees plays a determining role in the water balance of forest stands and in water yield from forested catchments and is a subject of increasing research interest, especially in regions such as where rainfall and temperatures are predicted to vary markedly in coming years (e.g. southeast Australia, Collins *et al*. 2011). Models of tree water use are important tools for forest and ecosystem managers in their efforts to predict ecosystem services, notably catchment water yield and carbon sequestration, in forested landscapes. Many such models, including those in current use, include limited representation of the biological control of transpiration (Running & Coughlan 1988; Rauscher *et al*. 1990; Korol, Running & Milner 1995; Leuning *et al*. 1995; Lloyd *et al*. 1995; Paruelo & Sala 1995; Jackson *et al*. 1998). It is still common (e.g. Granger & Pomeroy 1997; Pomeroy *et al*. 2007) for transpiration to be predicted solely by reference to the potential evaporation from a wet surface.

A summary of recent research (Levia, Carlyle-Moses & Tanaka 2011) strongly suggests that reliability and generality of such models under future climates may be greatly improved by incorporating current knowledge of the physiological mechanisms by which plants regulate transpiration. 'Bottom-up' modelling approaches – based on scaling up detailed leaf level models – are particularly needed to cope with the evident landscape-scale variation in stand-, site- and individual-scale biological properties that influence tree water use (Wilson *et al*. 2001; Ford *et al*. 2007). This must be weighed against the computational efficiency and ease of parameter estimation in 'top-down' approaches, which predict gas exchange using conservative properties (e.g. light use efficiency) that emerge at large scales from biological regulation at smaller scales, and which facilitate scaling up (Raupach & Finnigan 1988; Houborg *et al*. 2009). To be useful, models that predict the biological control of gas exchange must strike this balance – they should remain simple, yet able to capture wide biological variation and effects of climate change.

Closed form, process-based models of steady-state stomatal conductance have emerged in recent years (Jarvis & Davies 1998; Dewar 2002; Gao *et al*. 2002; Buckley, Mott & Farquhar 2003; Peak & Mott 2011) to complement widely used empirical models of stomatal conductance (Jarvis 1976; Ball, Woodrow & Berry 1987; Leuning 1995; Oren *et al*. 1999; White *et al*. 1999; Noe & Giersch 2004); for a review, see Damour *et al*. (2010). Because the parameters in these process models correspond to measurable biological and biophysical properties, they offer the prospect of more explicitly representing those properties, and more importantly their responses to environmental change, in bottom-up models. Yet in common use it is impractical to measure each of the parameters in these process models for application to large-scale predictions.

We show here that the 'BMF' process model of stomatal conductance (Buckley *et al*. 2003) can be reduced to a simpler form, with two to four 'lumped' parameters

Correspondence: T. N. Buckley. Fax: +1707 664 4046; e-mail: tom_buckley@alumni.jmu.edu

that still bear transparent relationships to the underlying biophysical parameters. The resulting model(s) offer a way to bridge the gap between empirical models that are computationally efficient and have few parameters, and detailed process models with many parameters. Our objectives were: (1) to develop robust but simplified models for stomatal conductance that were based on current understanding of stomatal conductance, as expressed in the BMF model; (2) to test those models against a number of independent sap flux datasets that encompassed considerable variation in environmental conditions and included two species and age classes; and (3) to show how the derived models can accommodate experimentally gained knowledge. For model testing and cross-validation, we used half-hourly and diurnally averaged sap flux data for 36 individual trees of two *Eucalyptus* species across seven forest stands in the mountains of southeastern Australia that varied in age (time since fire). Those datasets cover periods ranging from 176 to 365 d (average: 289 d).

MATERIALS AND METHODS

The BMF process-based model of stomatal conductance

The stomatal conductance model of Buckley *et al*. (2003) (BMF) can be expressed as

$$g_s = \frac{K_l(\psi_{soil} + \pi_e)}{K_l/\chi\alpha + D_s}, \quad (1)$$

where K_l is leaf-specific hydraulic conductance; ψ_{soil} is soil water potential (MPa); π_e is epidermal osmotic pressure; D_s is the water vapour mole fraction difference between the leaf's intercellular air spaces and the leaf surface (mmol mol^{-1}); χ is a scalar that relates conductance (g_s) to turgor pressures of epidermal and guard cells, and which includes the effect of stomatal density; and α is the 'guard cell advantage', which incorporates the effects of light, CO_2 and hormonal signals from roots (ABA) as well as an offset representing the epidermal mechanical advantage. (Table 1 defines symbols used in this study; symbols used only in the Appendix are defined there.) α is not a parameter, but rather a function of irradiance and intercellular CO_2 that includes additional parameters, and will be discussed further next.

Equation 1 is simplified from the original BMF model in two ways. Firstly, it assumes that the osmotic gradient from guard to epidermal cells, rather than from guard cells to the adjacent apoplast, is the target for active guard cell osmoregulation. This is consistent with other analyses (Dewar 2002; Franks & Farquhar 2007). Secondly, it assumes hydraulic resistance from epidermal to guard cells is negligible compared to that from soil to epidermal cells; this is open to debate (Dewar 1995; Peak & Mott 2011) but is supported by much circumstantial evidence (Buckley & Mott 2002; Buckley 2005).

Table 1. Parameters and variables referred to in the main text of this study, listed in alphabetical order

Name	Symbol	Units
Guard cell advantage	α	Unitless
α at saturating irradiance	α_m	Unitless
Lumped parameter, defined as $K_l/\chi\alpha_m$	b	mmol mol^{-1}
Turgor to conductance scalar	χ	mol m^{-2} s^{-1} MPa^{-1}
Air H_2O vapour pressure saturation deficit	D	mmol mol^{-1}
Leaf surface vapour pressure saturation deficit	D_s	mmol mol^{-1}
Maximum leaf transpiration rate	E_m	mmol m^{-2} s^{-1}
Initial slope of response of α to irradiance	ϕ	[μmol m^{-2} s^{-1}]$^{-1}$
Sap flux	f	cm^3 cm^{-2} h^{-1}
Maximum sap flux	f_m	cm^3 cm^{-2} h^{-1}
Stomatal conductance to water vapour	g_s	mol m^{-2} s^{-1}
Irradiance (photosynthetic photon flux)	i	μmol m^{-2} s^{-1}
α in darkness, divided by ϕ	i_o	μmol m^{-2} s^{-1}
Lumped parameter, defined as $K_l/\chi\phi$	k	μmol m^{-2} s^{-1} mmol mol^{-1}
Leaf specific hydraulic conductance	K_l	mmol m^{-2} s^{-1} MPa^{-1}
Epidermal osmotic pressure	π_e	MPa
Ratio of leaf area to sapwood area	σ	m^2 cm^{-2}
Soil water potential	ψ_{soil}	MPa

Deriving a simplified four-parameter conductance model from BMF

The major simplification that we apply to BMF in this study is to approximate the guard cell advantage, α, by a saturating hyperbolic function of photosynthetic photon flux density (irradiance, i):

$$\alpha = \frac{\alpha_m\phi(i + i_o)}{\alpha_m + \phi i}, \quad (2)$$

where α_m is the limit of α at high irradiance, and ϕ is the initial slope of α versus i. Figure 1 compares Eqn 2 with the model for α used by Buckley *et al*. (2003). The latter model was based on the mesophyll ATP concentration model of Farquhar & Wong (1984), which was in turn derived from the photosynthesis model of Farquhar, von Caemmerer & Berry (1980). In the full model for α, light saturation is reached more abruptly than in the hyperbolic model, but the general character of the response is similar. The original α model also captures responses to ambient CO_2 concentration (which we will address in the Discussion), and it has a negative offset to represent the epidermal mechanical advantage. Given it is now clear that stomata are often partly open in the dark, giving rise to nocturnal transpiration (Caird, Richards & Donovan 2007; Dawson *et al*. 2007), Eqn 2 includes a positive offset, i_o.

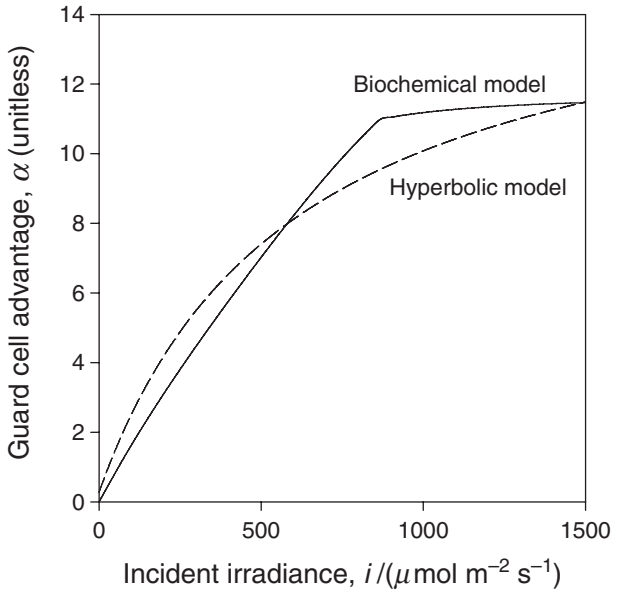

Figure 1. Comparison of two models for the response of guard cell advantage (α) to incident irradiance (i). Solid line ('biochemical model'): model used by Buckley *et al*. 2003), with photosynthetic parameters given by those authors. Dashed line ('hyperbolic model'): model used in this study (Eqn 2), with $i_o = 10$ μmol m^{-2} s^{-1}, $\alpha_m = 13$ and $\phi = 0.022$ (μmol m^{-2} s^{-1})$^{-1}$.

Substituting Eqn 2 in Eqn 1 leads to:

$$g_s = \frac{K_l(\psi_{soil} + \pi_e)(i + i_o)}{\frac{K_l}{\chi\phi} + \frac{K_l}{\chi\alpha_m} i + (i + i_o) D_s}. \quad (3)$$

We may group parameters by defining $E_m = K_l(\psi_{soil} + \pi_e)$, $k = K_l/\chi\phi$ and $b = K_l/\chi\alpha_m$. This gives

$$g_s = \frac{E_m(i + i_o)}{k + bi + (i + i_o) D_s}. \quad \text{(Model 4)} \quad (4)$$

We chose the symbol E_m because $K_l(\psi_{soil} + \pi_e)$ is the maximum transpiration rate at large D_s (see the Appendix). We call Eqn 4 'Model 4' because it has four parameters (E_m, k, b and i_o). Technically, of course, there are seven parameters (K_l, ψ_{soil}, π_e, i_o, χ, ϕ and α_m). However, preliminary results from applying this model to one of our datasets suggested that treating E_m, k, b and i_o as invariant parameters on seasonal time scales led to surprisingly accurate predictions for our study systems, motivating the broader tests presented here. Model 4 can be thought of as a simplified expression of the BMF model, constrained by the hypothesis of invariance of these 'lumped' parameters.

Two- and three-parameter alternative models

To determine the simplest model (in the sense of having the fewest parameters) capable of adequately predicting g_s, we will now derive a suite of alternative models based on Model 4. The first arises by assuming that $\phi i << \alpha_m$ ($bi << k$); that is, that the stomatal response to irradiance is typically in the approximately linear region at low irradiance. This yields $\alpha \approx \phi(i + i_o)$ in place of Eqn 2. Although Eqn 2 actually predicts large curvature in α vs i at low irradiance, the photosynthesis-based model for α originally used by Buckley *et al*. (2003) is more nearly linear at low irradiance (Fig. 1), so the approximation merits testing as a predictive tool. This gives:

$$g_s = \frac{E_m(i + i_o)}{k + (i + i_o) D_s}. \quad \text{(Model 3)} \quad (5)$$

Alternative models suitable for predictions at diurnal rather than half-hourly time scales may be obtained by eliminating i_o, because this parameter is only needed to predict nocturnal transpiration. Setting i_o equal to zero gives:

$$g_s = \frac{E_m i}{k + bi + iD_s}, \quad \text{(Model 4d)} \quad (6)$$

$$g_s = \frac{E_m i}{k + iD_s}, \quad \text{(Model 3d)} \quad (7)$$

The models' names are appended with 'd' in Eqns 6 and 7 to indicate that they are only meant to apply at diurnal time scales.

Testing the models

We tested the models above by using them to predict whole tree sap flux (f, cm^3 cm^{-2} h^{-1}), as

$$f = 64.9\sigma D g_s(i, D), \quad (8)$$

where 64.9 [(cm^3 h^{-1})/(mmol s^{-1})] is a unit conversion, σ is the ratio of leaf area to sapwood area (m^2 cm^{-2}), D is the water vapour mole fraction saturation deficit of the air (mmol mol^{-1}), and $g_s(i,D)$ is the conductance predicted from Eqns 4–7 using measurements of i and D. Applying Eqn 8 to the models modifies the parameter E_m, such that the parameter we actually estimated is maximum sap flux (f_m), which is related to E_m by

$$f_m = (64.9\sigma) E_m. \quad (9)$$

We estimated f_m, k, b and i_o by fitting the models to our sap flux data in cross-validation analysis (see *Model fitting and testing* for details), and compared fitted estimates of f_m with actual maximum values of f in each dataset; inference of E_m from f_m requires estimates of σ, which were not available. Note that replacing D_s with D requires that the canopy is well coupled aerodynamically, so that D_s and D are similar and uniform through the canopy. Aerodynamic decoupling is unlikely for our study sites, which are in open woodlands or tall open forests and have relatively low leaf area indices; a recent study in these sites (Buckley *et al*. 2011) found no

consistent effect of wind speed on canopy conductance, indicating a high degree of coupling.

Sap flux and environmental measurements

We measured sap flux (f) in 36 trees: five to six trees at each of seven sites, listed in Table 2. Two species were sampled: *Eucalyptus delegatensis* and *Eucalyptus pauciflora*. Three of the seven sites (two for *E. delegatensis* and one for *E. pauciflora*) were in 6 to 8-year-old stands that germinated (*E. delegatensis*) or resprouted (*E. pauciflora*) after fires in 2003 killed mature stands at those sites. The other four sites were in nearby mature stands that survived the fires. The mature *E. delegatensis* sites were 71 years old and approximately 40–50 m in height. The age of the mature *E. pauciflora* sites is unknown, and tree age may range from 45 years (most likely, due to fires 45 years ago) to several hundred years; these stands are approximately 10–15 m in height. Sap flux was measured every 30 min by the HRM method (Burgess *et al*. 2001; Bleby, Burgess & Adams 2004) using one sap flux probe set (ICT International, Armidale, NSW, Australia) installed at 1.3 m height in each stem at a consistent azimuth in each site. Probe sets included outer and inner probes, at 12.5 and 27.5 mm depths, respectively. Additional details of sap flux measurements procedures are given by Buckley *et al*. (2011). Whole tree sap flux, f, was calculated as the sum of the products of sapwood area and sap flux for outer and inner sapwood regions, all divided by total sapwood area. Sapwood regions were delineated by a boundary corresponding to the midpoint between the inner and outer probes. Outer sapwood area was taken as the lesser of total sapwood area (calculated from sapwood length in two cores per tree) and the area of the outer region; inner sapwood area was the remainder of total sapwood area.

Table 2. Metadata for sites and data records used to test the sap flux models in this study

Tree	DBH	SA	Days	Period of data record
E. delegatensis, mature				
Dm1_1	44.0	280.8	365	10 August 2009–09 August 2010
Dm1_2	45.0	220.9	365	10 August 2009–09 August 2010
Dm1_3	66.3	514.6	365	10 August 2009–09 August 2010
Dm1_4	52.5	303.6	365	10 August 2009–09 August 2010
Dm1_5	35.8	174.0	365	10 August 2009–09 August 2010
Dm1_6	58.5	371.4	365	10 August 2009–09 August 2010
Dm2_2	61.3	447.8	331	09 August 2009–08 August 2010
Dm2_3	76.4	578.7	331	09 August 2009–08 August 2010
Dm2_4	48.2	176.1	331	09 August 2009–08 August 2010
Dm2_5	53.0	320.7	301	09 August 2009–09 July 2010
Dm2_6	44.1	204.0	331	09 August 2009–08 August 2010
E. delegatensis, regrowth				
Dr1_1	11.0	53.0	365	09 August 2009–08 August 2010
Dr1_2	9.5	44.9	365	09 August 2009–08 August 2010
Dr1_3	9.0	39.3	365	09 August 2009–08 August 2010
Dr1_4	11.0	62.9	364	09 August 2009–07 August 2010
Dr1_5	9.0	45.9	365	09 August 2009–08 August 2010
Dr2_1	9.2	31.2	348	09 August 2009–25 August 2010
Dr2_2	10.4	50.1	349	09 August 2009–25 August 2010
Dr2_3	10.7	44.7	233	02 December 2009–25 August 2010
Dr2_4	10.1	37.4	348	09 August 2009–25 August 2010
Dr2_5	10.1	48.5	233	02 December 2009–25 August 2010
E. pauciflora, mature				
Pm1_1	29.0	171.6	176	21 October 2008–14 April 2009
Pm1_2	18.5	73.1	176	21 October 2008–14 April 2009
Pm1_4	21.0	121.7	176	21 October 2008–14 April 2009
Pm1_5	24.0	107.8	176	21 October 2008–14 April 2009
Pm1_6	27.0	151.4	176	21 October 2008–14 April 2009
Pm2_1	21.0	69.7	181	18 November 2009–20 May 2010
Pm2_2	29.0	142.4	181	18 November 2009–20 May 2010
Pm2_3	57.1	238.1	181	18 November 2009–20 May 2010
Pm2_4	35.6	203.0	181	18 November 2009–20 May 2010
Pm2_5	41.3	335.3	181	18 November 2009–20 May 2010
E. pauciflora, regrowth				
Pr2_1	5.3	12.2	184	18 November 2009–20 May 2010
Pr2_2	6.7	24.5	183	20 May 2009–18 November 2009
Pr2_3	4.9	12.1	365	20 May 2009–19 May 2010
Pr2_4	5.4	14.9	184	20 May 2009–19 November 2009
Pr2_5	5.3	15.7	365	20 May 2009–19 May 2010

DBH, cm; SA, total sapwood area, cm^2; days, number of days in the data record; period, time span of the data record. Capital letters in tree codes denote species (D, *E. delegatensis*; P, *E. pauciflora*); lowercase letters denote age class (m, mature; r, post-2003-fire regrowth), and the first number identifies the site.

Air water vapour mole fraction saturation deficit (D, mmol mol^{-1}) was calculated from air temperature and relative humidity, measured using sensors (HT-1, ICT International) installed within each site. Photosynthetic photon flux density (i) was measured by sensors (PAR Smart Sensor, Onset Corp, Pohansett, MA, USA) in automatic weather stations near each site. To test Models 3d and 4d, diurnal averages of f were computed for the period of non-zero i in each 24 h period.

Model fitting and testing

All model fitting and testing was performed in Mathematica 8.0.4.0 (Wolfram Research Inc., Champaign, IL, USA) using the 'NonlinearModelFit' function for fitting the models and computing statistical parameters of the fit, the 'LinearModelFit' function for regression analysis of residuals, and code written by the authors for all other computations. Preliminary analysis yielded best-fit parameters for one site, and those parameters were subsequently used as initial parameter values for NonlinearModelFit.

Stationary cross-validation

We quantified the goodness of fit and predictive power of the models (Eqns 4–7) based on output from stationary cross-validation (SCV). In each test, a random sample of one half of the data for a particular tree (the 'training data') was used to fit the model, and the remainder of the data (the 'testing data') were used to test the fitted model. The entire procedure was repeated 100 times for each tree. This is equivalent to 100-fold cross-validation with randomized selection of training data, or Monte Carlo cross validation with 100 iterations (Burman 1989; Arlot & Celisse 2010).

Each series of SCVs was repeated twice: once using half-hourly data with Models 3 and 4, and once using diurnally averaged data with Models 3d and 4d. [We also performed non-stationary cross validation (NSCV), described next.]

We quantified the models' goodness of fit in three different ways for each SCV run, based on aspects of the fit between the models and the training data.

1. To describe the fit and characterise its overall quality, we recorded best fit parameter values and *P*-values for each parameter.
2. To detect any systematic deviation of the model from the data, we performed multiple linear regression on residuals of the fitted model from the training data with *i, D* and time (*t*) as independent variables, and recorded standardized regression slopes for significant effects ($P < 0.05$).
3. To assess the relative parsimony of the models, we compared values of the corrected Akaike Information Criterion (AICc) and Bayes Information Criterion (BIC) computed for each fit (Arlot & Celisse 2010); smaller values for these parameters indicate greater parsimony. For each of these outputs, we report medians and median absolute deviations (MADs) among trees in each species/age class group, rather than means and standard errors, which are less robust to outliers (Staudte & Sheather 1990).

We quantified the predictive power of the fitted models in three different ways.

1. Firstly, we used *F*-tests to determine whether the intercepts and slopes of predicted versus measured flux were significantly different from zero and unity, respectively.
2. Secondly, we recorded r^2 for the relationship between measured and predicted sap flux in each SCV run, and computed the median r^2 among runs.
3. These r^2 values quantify the models' overall predictive accuracy. However, they overstate the *gain* in accuracy obtained by modelling stomatal control *per se*, because the null model implicit in r^2 is constant sap flux (the denominator of r^2 is the sum of squares of $f - f_{avg}$, where f_{avg} is the mean of f in the testing data). Therefore, we computed a second, modified version of r^2 (denoted r^2_g, Eqn 10) in which the null model assumed constant *conductance* (i.e. $f = GD$ where G is a constant; Eqn 11) rather than constant flux:

$$r^2_{\mathrm{g}} = 1 - \sum_i (f_{\mathrm{i}} - f_{\mathrm{model,i}})^2 \Big/ \sum_i (f_{\mathrm{i}} - f_{\mathrm{null,i}})^2, \quad (10)$$

$$f_{\mathrm{null}} = GD, \quad (11)$$

where f_{i} is measured sap flux for time point i in the testing data, $f_{\mathrm{model,i}}$ is the corresponding model prediction and $f_{\mathrm{null,i}}$ is the prediction from Eqn 11. The parameter G in Eqn 11 was found by fitting Eqn 11 to the training data. Equation 10 gives the fraction of *conductance-related* variation in sap flux explained by the models.

NSCV

Traditional cross-validation using time series data can be uninformative because of temporal trends in the process being modelled (Arlot & Celisse 2010; Bergmeir & Benîtez 2012). To detect changes over time in the nature of the model fit and its predictive power, we also performed NSCVs, in which the training data comprised 1 month (28 successive days), and the testing data comprised the remainder of the dataset. This was iterated, with the 28 d 'training window' advanced by increments of 1 week, until the training window reached the end of the dataset. This is equivalent to 'leave-*k*-out cross validation' (Arlot & Celisse 2010) with k equal to 28 d (28 or 1344 data points for diurnally averaged or half-hourly data, respectively). We omitted results from runs in which the training window spanned a data gap of longer than 7 d. In each run, we recorded r^2 values for testing data versus fitted models as a measure of the ability of parameter sets estimated in one narrow window of time to predict sap flux at other times in the dataset.

RESULTS

SCV of Models 3 and 4 (half-hourly data)

Both models predicted half-hourly sap flux well (Figs 2 & 3), and reproduced most absolute and conductance-related variation in observed sap flux in SCV. Over all trees, Models 4 and 3 predicted 86 and 83% of total variation in sap flux, respectively (r^2, Table 3), and 76 and 73% of conductance-related variation (r^2_g, Table 3). Slopes of predicted versus measured flux differed significantly from unity in only 3–5 of 36 trees for each model; intercepts differed from zero in 31 of 36 trees for both models, but median intercepts (standardized by mean flux) were small: 0.05 and 0.04 for Models 4 and 3, respectively. In most trees, residuals (data minus model) were positively correlated with irradiance for Model 4 and negatively for Model 3; residuals were mostly negatively correlated with *D* for Model 4 and positively for Model 3 (Table 4). This suggests that Model 4 tends to underestimate sap flux at high irradiance and low evaporative demand (VPD), and the reverse is true for Model 3. However, median standardized slopes for these residuals ranged in magnitude from 0.07 to 0.11, with median regression $r^2 = 0.02$ (Model 4) and 0.04 (Model 3), indicating very weak correlations whose significance was magnified by the very large sample size (n = 8448–17 520). Model 4 was more parsimonious than Model 3 despite its additional parameter: AICc was lower for Model 4 in all trees, and BIC was lower in all but two trees (Table 3). All parameters were significant for both models for every tree.

SCV of Models 3d and 4d (diurnally averaged data)

Both models predicted diurnal average sap flux well (Figs 4 & 5): over all trees, Models 4d and 3d both predicted a

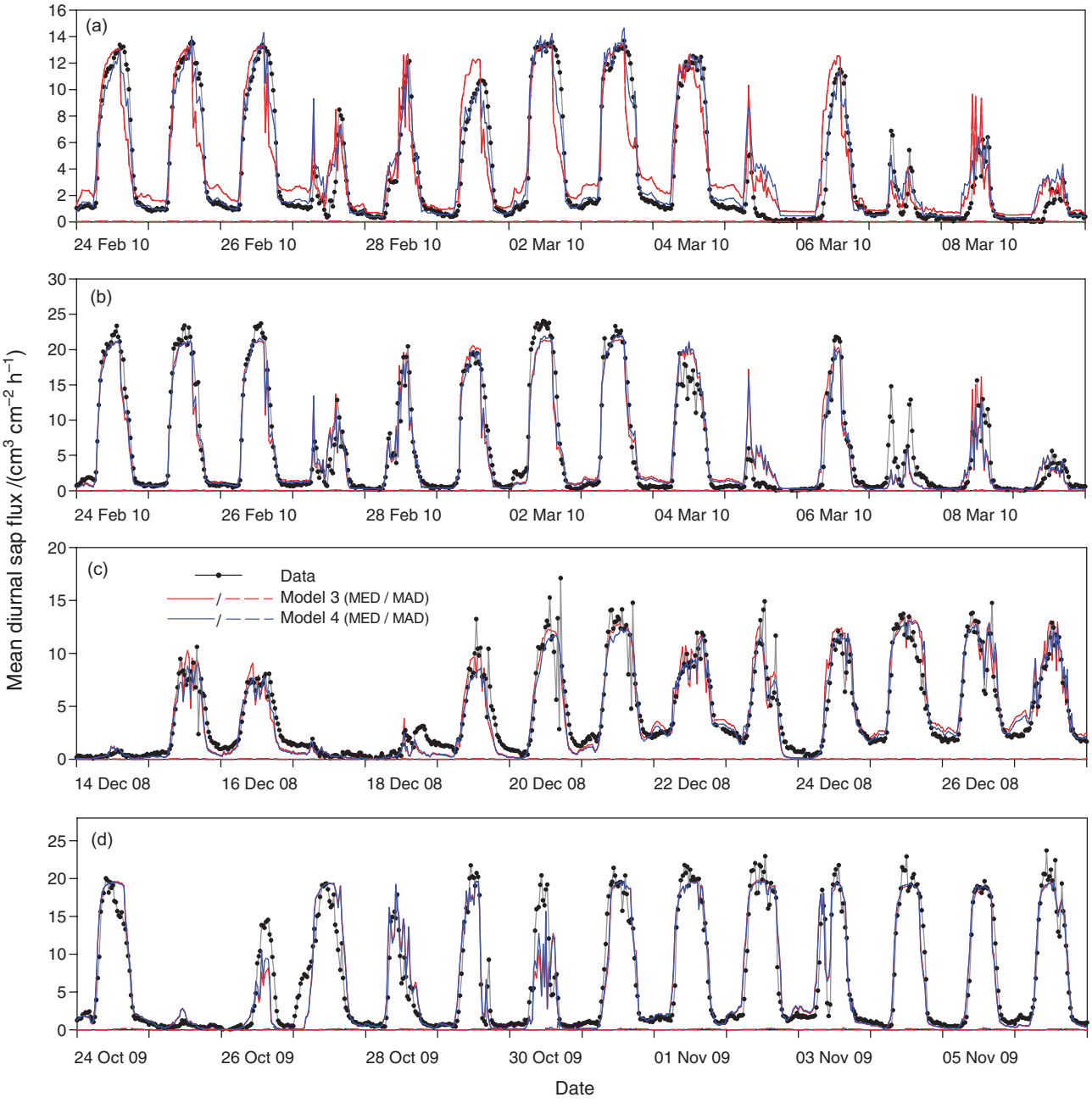

Figure 2. Representative time courses of half-hourly sap flux (black lines and symbols) and corresponding median predictions (MED) from Models 3 (red lines) and 4 (blue lines), for one tree in each species/age class group: (a) tree Dm1_1 (*E. delegatensis*, mature); (b) tree Dr2_4 (*E. delegatensis*, regrowth); (c) tree Pm1_6 (*E. pauciflora*, mature); (d) tree Pr2_4 (*E. pauciflora*, regrowth). Median absolute deviations (MADs) of predictions among cross-validation runs are shown with dashed lines.

median 89% of total variation in sap flux, and 78% of conductance-related variation (r^2 and r^2_g, Table 5). Slopes of predicted versus measured flux did not differ from unity in any tree, for either model. Intercepts differed from zero in 12 trees for Model 4d and in 17 trees for Model 3d (Table 4); in all but 4 of these 29 cases, this occurred in regrowth trees. Inspection of these relationships (Figs 4 & 5) suggests that the cause was a tendency for predicted flux to saturate at very high values of measured flux for the younger trees, particularly in *E. pauciflora*. Furthermore, for Model 3d, residuals were negatively correlated with i in 13 trees and positively with D in 8 (Table 4), indicating a moderate tendency to overestimate conductance at high light and underestimate it at high D. For Model 4d, residuals were correlated with D and with i in only three trees each (Table 4).

Model 4d showed a clear tendency for overfitting: Model 3d was more parsimonious in about two thirds of trees

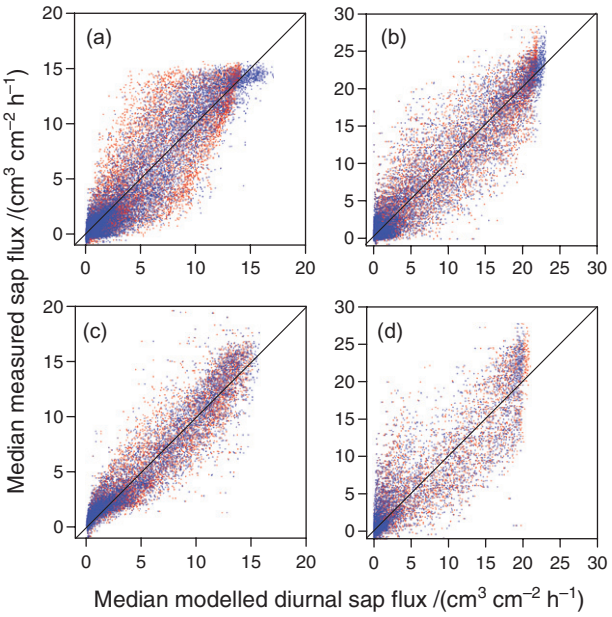

Figure 3. Representative plots of half-hourly sap flux versus median predictions from Model 3 (red points) or Model 4 (blue points) for one tree in each species/age class group: (a) tree Dm1_1 (*E. delegatensis*, mature); (b) tree Dr2_4 (*E. delegatensis*, regrowth); (c) tree Pm1_6 (*E. pauciflora*, mature); (d) tree Pr2_4 (*E. pauciflora*, regrowth). 1:1 lines are shown in each plot.

(18–25 out of 36; AICc and BIC, Table 3), the parameter b was insignificant in 23 of 36 trees and negative in 12 of 36 trees, and median r^2 was lower for Model 4d in 16 of 36 trees – all suggesting that the additional parameter in Model 4d tended to capture random features of the training data that were absent in the testing data.

Seasonal trends in model performance

Residuals were correlated with time in 27 of 36 trees for both half-hourly models, and in 22 of 36 trees for both diurnal models (Table 4). The absolute values of median standardized regression slopes for time were 0.06–0.07 for half-hourly data, and 0.06 (Model 3d) and 0.16 (Model 4d) for diurnally averaged data. This indicates a small but systematic seasonal bias when the models are used with constant parameters. Inspection of seasonal sap flux time-courses (Fig. 4) suggests that the models tend to underestimate conductance under conditions promoting very high flux in late spring or summer, and to overestimate flux in winter. Results from NSCV (Fig. 6) suggest that the models generally performed similarly whether parameters were estimated during 1 month in spring or autumn, or using a random sample of data from across the dataset (as in SCV). In all cases, parameters estimated in winter (June–August in Australia) performed very poorly; in *E. delegatensis*, model performance also declined using parameters estimated in summer, though to a lesser degree.

Parameter values

The parameter f_m, maximum sap flux, was broadly similar between species/age class groups, with median values ranging from 15.2 to 28.8 $cm^3\ cm^{-2}\ h^{-1}$ for half-hourly data and from 10.2 to 14.0 $cm^3\ cm^{-2}\ h^{-1}$ for diurnally averaged data (Tables 6 & 7). Fitted f_m values for the diurnal models compared well with actual f_m measured in each dataset, but fitted values for the half-hourly models tended to underestimate actual f_m (Fig. 7). Median fitted values of k and b varied more, ranging from 540 to 4940 $\mu mol\ m^{-2}\ s^{-1}$ mmol mol^{-1} and –1 to 5 mmol mol^{-1}, respectively, across models. The parameter i_o (Models 4 and 3 only) ranged from 5.9 to 123 $\mu mol\ m^{-2}\ s^{-1}$, and was typically greater in *E. pauciflora*: for Model 4, the more parsimonious of the two, median i_o was 5.9–6.9 $\mu mol\ m^{-2}\ s^{-1}$ for *E. delegatensis* versus 37–47 $\mu mol\ m^{-2}\ s^{-1}$ for *E. pauciflora*. These values correspond to approximately 0.3 and 2% of midday summer irradiance, respectively.

DISCUSSION

The stomatal conductance models developed here provided robust predictions of sap flux. For half-hourly data that included nocturnal periods, Model 4 was more parsimonious (lower AICc and BIC) and more consistently accurate (higher r^2) than Model 3 for 32 of 36 trees. Even in trees

Table 3. Coefficients of determination (r^2, r^2_g) for relationships between half-hourly testing data and fitted models (Models 3 and 4), and fractions of trees in which Model 3 was judged more parsimonious than Model 4 (based on smaller AICc or BIC)

	r^2		r^2_g			
Group	Model 4	Model 3	Model 4	Model 3	*AICc3 < AICc4?*	*BIC3 < BIC4?*
E. delegatensis (M)	0.88 ± 0.03	0.82 ± 0.01	0.78 ± 0.04	0.66 ± 0.05	1/11	1/11
E. delegatensis (R)	0.88 ± 0.03	0.88 ± 0.05	0.81 ± 0.07	0.80 ± 0.09	0	1/10
E. pauciflora (M)	0.82 ± 0.04	0.81 ± 0.03	0.73 ± 0.03	0.72 ± 0.04	0	0
E. pauciflora (R)	0.84 ± 0.02	0.84 ± 0.03	0.64 ± 0.10	0.64 ± 0.08	0	2/5
All trees	0.86 ± 0.03	0.83 ± 0.03	0.76 ± 0.06	0.73 ± 0.06	1/36	4/36

r^2 and r^2_g indicate the fraction of variance in sap flux explained by the models, relative to null models of constant sap flux (r^2) or constant conductance (r^2_g), respectively. Values shown are medians ± median absolute deviations among trees in each group.
AICc, Akaike Information Criterion; BIC, Bayes Information Criterion; M, mature; R, regrowth.

Table 4. Standardized regression coefficients from multiple regressions of residuals (testing data minus fitted model) versus irradiance (i), evaporative demand (D) and time (t)

Group/model	i	D	t
Model 4			
E. delegatensis (M)	0.05 (11/11)	–0.13 (10/11)	–0.14 (7/11)
E. delegatensis (R)	0.08 (8/10)	–0.07 (9/10)	0.13 (7/10)
E. pauciflora (M)	0.04 (3/10)	–0.11 (9/10)	0.07 (8/10)
E. pauciflora (R)	0.08 (4/5)	–0.08 (5/5)	0.10 (4/5)
All trees	0.07 (26/36)	–0.09 (33/36)	0.07 (26/36)
Model 3			
E. delegatensis (M)	–0.20 (11/11)	0.17 (11/11)	–0.11 (7/11)
E. delegatensis (R)	–0.08 (7/10)	0.12 (9/10)	0.13 (7/10)
E. pauciflora (M)	–0.10 (10/10)	0.001 (8/10)	0.07 (8/10)
E. pauciflora (R)	0.11 (5/5)	–0.18 (5/5)	0.12 (4/5)
All trees	–0.11 (33/36)	0.08 (33/36)	0.06 (26/36)
Model 4d			
E. delegatensis (M)	–	–0.41 (3/11)	0.41 (8/11)
E. delegatensis (R)	0.35 (2/10)	–	0.003 (5/10)
E. pauciflora (M)	0.35 (1/10)	–	0.48 (5/10)
E. pauciflora (R)	–	–	0.02 (3/5)
All trees	0.34 (3/36)	–0.41 (3/36)	0.16 (21/36)
Model 3d			
E. delegatensis (M)	–0.33 (8/11)	0.25 (4/11)	0.28 (9/11)
E. delegatensis (R)	0.31 (1/10)	0.32 (1/10)	0.01 (5/10)
E. pauciflora (M)	–0.42 (5/10)	0.25 (2/10)	0.11 (5/10)
E. pauciflora (R)	–	–0.35 (1/5)	0.04 (3/5)
All trees	–0.38 (14/36)	0.25 (8/36)	0.06 (22/36)

Values shown are medians among significant slopes in each group. Numbers in parentheses are fractions of trees in each group for which coefficients were significant ($P < 0.05$). Where values are missing, slopes were insignificant for all trees.
M, mature; R, regrowth.

where Model 3 was more parsimonious, Model 4 improved the accuracy of diel time courses of sap flux by better capturing the range between nocturnal minimum and diurnal maximum sap flux (e.g. Fig. 2a). That improvement is largely due to Model 4 accounting for saturation in the response of stomatal conductance to irradiance. Model 4 also described nocturnal transpiration well, by assuming persistent nocturnal stimulation of guard cell osmotic pressure equivalent to a median 'dark irradiance' (the parameter i_o) of 8.5 μmol m^{-2} s^{-1} or about 0.5% of midday summer irradiance. We conclude that Model 4 is preferable to Model 3 for predicting diel variations in g_s.

The opposite was true for diurnally averaged data. Model 3d was more parsimonious and more accurate in cross-validation than Model 4d in most trees, and Model 4d was not visibly superior to Model 3d in any dataset. The omission of nocturnal data reduced the range of irradiance in these datasets, and with it, the need to account for saturation in the stomatal response to irradiance – the main advantage of Model 4d over 3d. We conclude that Model 3d is at least as suitable as Model 4d for predicting diurnally averaged sap flux, and perhaps more so, because with only two parameters, Model 3d has greater potential for wide application.

Sap flux predicted by the models was generally higher than observed in winter, and slightly lower in spring. We expected the reverse, because the models – as tested here, using constant values for all parameters across seasons – did not explicitly account for changes in soil water potential, which is embedded in the parameter E_m (f_m as applied to our data). Soil moisture typically falls in summer and rises in winter, and this is widely thought to be an important influence on stomatal conductance. The fact that assuming constant E_m did not cause overestimation of flux in summer may reflect osmotic adjustment: E_m is defined as $K_l(\psi_{soil} + \pi_e)$, so changes in ψ_{soil} over weeks or months could be counterbalanced by increases in leaf osmotic pressure, π, preventing E_m from declining (Morgan 1984). Eucalypts are known for such adjustment (e.g. Arndt *et al*. 2008; Merchant *et al*. 2010). It is unclear why g_s should actually be *less* than predicted in winter, although temperature effects and fluctuations in sapwood to leaf area ratio (σ, Eqn 9) are likely explanations. We did not attempt to include temperature effects directly into our models, but they could be accommodated via changes in the parameters α_m and K_l in similar manner as we show in the Appendix (and discussed next) for effects of CO_2 enrichment on those parameters. That is beyond the scope of the present study. Changes in σ are only relevant in the context of using sap flux data to test our conductance models, so they do not bear on our models' ability to predict conductance. For now, we note that with fixed parameters, the models were able to predict sap flux well across multiple seasons. The models would remain useful even if parameters were estimated separately for summer and winter.

Although Models 3d and 4d cannot predict nocturnal transpiration, it may be possible to compensate for this with little increase in uncertainty. Recent studies suggest that

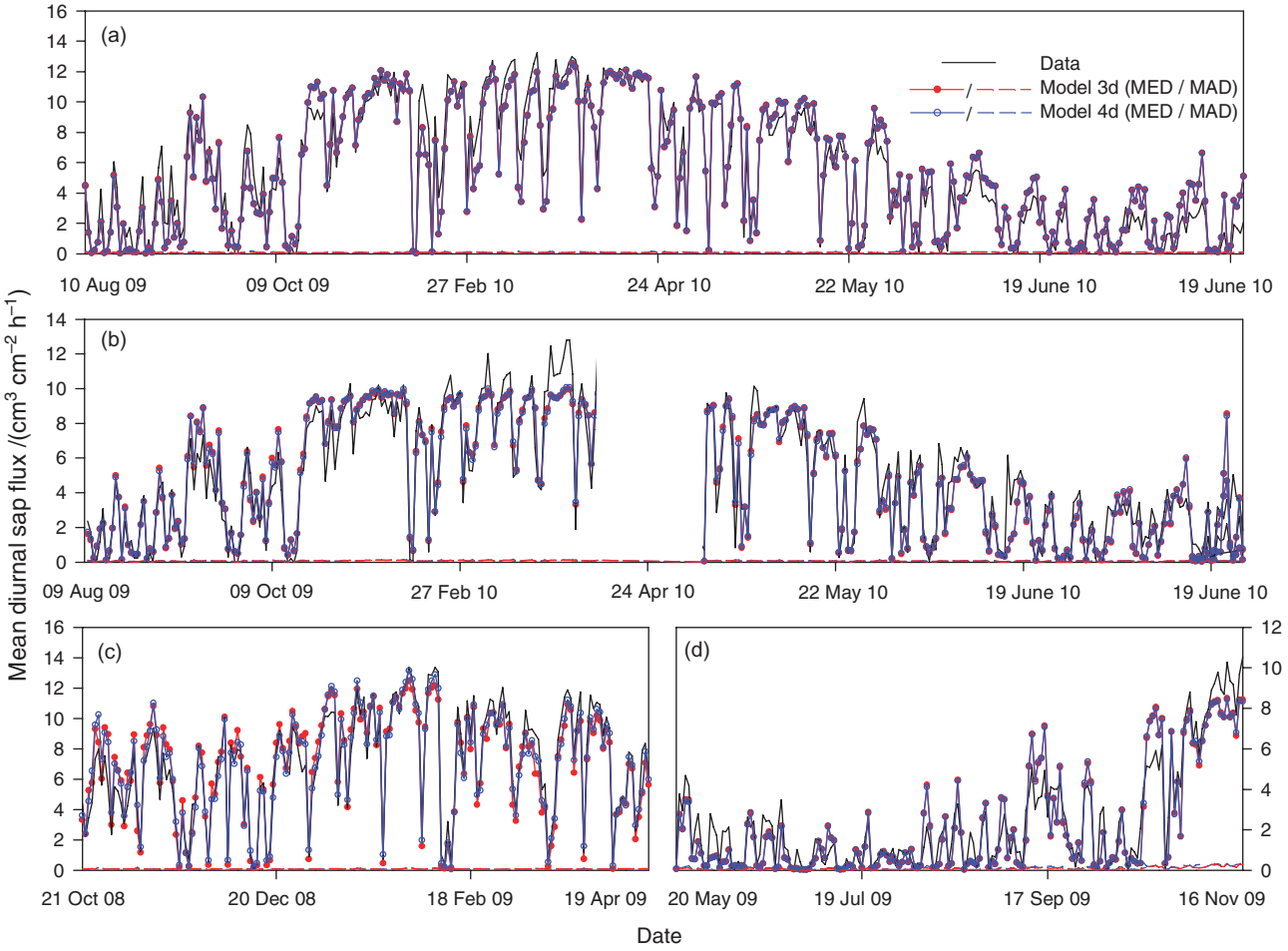

Figure 4. Representative time courses of diurnally averaged sap flux (solid line) and corresponding median predictions from Models 3d (red line, closed symbols) and 4d (blue line, open symbols), for one tree in each species/age class group: (a) tree Dm1_1 (*E. delegatensis*, mature); (b) tree Dr2_4 (*E. delegatensis*, regrowth); (c) tree Pm1_6 (*E. pauciflora*, mature); (d) tree Pr2_4 (*E. pauciflora*, regrowth). Median absolute deviations (MADs) of predictions among cross-validation runs are shown with dashed lines.

nocturnal transpiration in native Australian tree species tends to be between 6 and 10% of diel totals, and that this fraction does not vary greatly between seasons (Phillips *et al*. 2010; Zeppel *et al*. 2010; Buckley *et al*. 2011). This suggests that Model 3d or 4d could be used with a correction factor of approximately 1.06–1.10 to account for nocturnal losses.

Our models can accommodate new knowledge and generate testable hypotheses

The utility of the models tested in this study is enhanced by their parameters being explicitly related to reduced properties and processes, as embodied in the BMF model (Buckley *et al*. 2003). This allows experimental knowledge of how the physiological parameters in the BMF model respond to long-term environmental change, including climate change, to be directly applied to our models. For example, a wealth of data is now available concerning effects of CO_2 enrichment on photosynthetic parameters and stomatal conductance. The parameters α_m and ϕ can be related to photosynthesis-related parameters in the original model of guard cell advantage (α) used by Buckley *et al*. (2003); in the Appendix, we develop these relationships and then apply results of a meta-analysis of CO_2 enrichment experiments (Ainsworth & Long 2005) to show that α_m, ϕ and guard cell advantage, α, are predicted to decline by about 10, 19 and 15%, respectively, with a 200 μmol mol^{-1} increase in ambient CO_2. We can apply these predicted changes to Eqn 1 to estimate the change in g_s. Assuming ψ_{soil} and π are unaffected by enrichment, then

$$\frac{g_s'}{g_s} = \frac{K_l'}{K_l'/\chi\alpha' + D}\left(\frac{K_l/\chi\alpha + D}{K_l}\right), \qquad (12)$$

where primes denote values at elevated CO_2. This shows that the effect of changes in photosynthesis-related factors (captured by α), is mediated by hydraulic supply and demand (captured by K_l and D). Note that g_s'/g_s approaches α'/α at low D, and K_l'/K_l at high D. Thus, in the limit of low

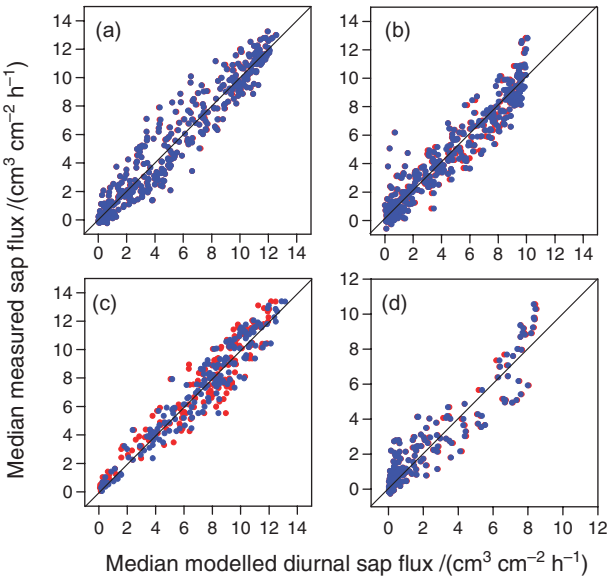

Figure 5. Representative plots of diurnally averaged sap flux versus median flux predictions from Model 3d (red points) or Model 4d (blue points) for one tree in each species/age class group: (a) tree Dm1_1 (*E. delegatensis*, mature); (b) tree Dr2_4 (*E. delegatensis*, regrowth); (c) tree Pm1_6 (*E. pauciflora*, mature); (d) tree Pr2_4 (*E. pauciflora*, regrowth). 1:1 lines are shown in each plot.

D, CO_2 enrichment is predicted to reduce g_s by 15%. Effects of enrichment on K_l have not been characterized as thoroughly as photosynthetic responses, but available data suggest that K_l often declines in trees grown under CO_2 enrichment. For example, Domec *et al.* (2009) reported a 14–22% decline in leaf hydraulic conductance in response to enrichment in *Pinus taeda*, and Heath, Kerstiens & Tyree (1997) found a 21% decline in K_l in oak. If K_l and α both decline by around 15%, then g_s is predicted to decline by 15% at all D. This compares well with the average reduction of 15.6% among tree species in free-air CO_2 enrichment (FACE) experiments reported by Ainsworth & Long (2005). However, Heath *et al.* (1997) found no decline in K_l or midday g_s during summer drought in beech – when evaporative demand is high – and similarly, Tognetti *et al.* (1998) reported little change in g_s and in fact an increase in K_l during summer drought in oak. These results are also consistent with our analysis, as Eqn 12 suggests that changes in K_l dominate the effect of enrichment on g_s under high evaporative demand.

Comparison with other simple models of the biological control of transpiration

Other simple models exist for stomatal control of plant water loss. Perhaps the most widely used are formulations related to the Jarvis (1976) and Ball–Berry models (Ball *et al.* 1987), which have been applied to many tree, canopy and landscape models (e.g. Running & Coughlan 1988; Collatz *et al.* 1991; Van Wijk *et al.* 2000; Reichstein *et al.* 2002; Battaglia *et al.* 2004). Jarvis-type models consist of several multiplicative unit adjustment factors, each accounting for a different environmental influence on stomatal conductance. Although the Jarvis approach is conceptually simple and modular, it assumes the many controls on stomatal conductance act independently, which is not supported by current knowledge of stomatal physiology (Buckley 2005). Leuning (1995) modified Ball–Berry to better represent improved knowledge about stomatal physiology, and the resulting 'BBL' model shares some structural features with BMF. However, the structures of the BBL and BMF models differ in important ways. Firstly, BBL captures nocturnal water loss with a non-zero intercept for stomatal conductance, which does not accommodate recent studies showing that stomata remain sensitive to VPD at night (Barbour & Buckley 2007; Cavender-Bares, Sack & Savage 2007); our models capture that behaviour. Secondly, BBL captures the tendencies for g_s to track photosynthetic capacity among leaves and plants, and photosynthetic rate over time for a given leaf, by setting g_s to be directly proportional to net CO_2 assimilation rate. This requires a full model for net photosynthetic rate, which adds complexity and parameter estimation requirements that are unnecessary in many applications. Our models achieve the same outcome but in a different way: the short-term coordination of g_s with photosynthesis is captured via the response of guard cell advantage, α, to irradiance, i (Eqn 2).

Table 5. Coefficients of determination (r^2, r^2_g) for relationships between diurnally averaged testing data and fitted models (Models 3d and 4d), and fractions of trees in which Model 3d was judged more parsimonious than Model 4d (based on smaller AICc or BIC)

	r^2		r^2_g			
Group	Model 4d	Model 3d	Model 4d	Model 3d	*AICc3 < AICc4?*	*BIC3 < BIC4?*
E. delegatensis (M)	0.92 ± 0.06	0.92 ± 0.06	0.82 ± 0.11	0.79 ± 0.11	3/11	6/11
E. delegatensis (R)	0.87 ± 0.03	0.87 ± 0.03	0.76 ± 0.06	0.76 ± 0.06	8/10	10/10
E. pauciflora (M)	0.86 ± 0.08	0.86 ± 0.07	0.79 ± 0.11	0.76 ± 0.07	4/10	6/10
E. pauciflora (R)	0.85 ± 0.04	0.86 ± 0.04	0.60 ± 0.14	0.61 ± 0.14	3/5	4/5
All trees	0.89 ± 0.05	0.89 ± 0.05	0.78 ± 0.10	0.78 ± 0.08	18/36	25/36

r^2 and r^2_g indicate the fraction of variance in sap flux explained by the models, relative to null models of constant sap flux (r^2) or constant conductance (r^2_g), respectively. Values shown are medians ± median absolute deviations among trees in each group.
AICc, Akaike Information Criterion; BIC, Bayes Information Criterion; M, mature; R, regrowth.

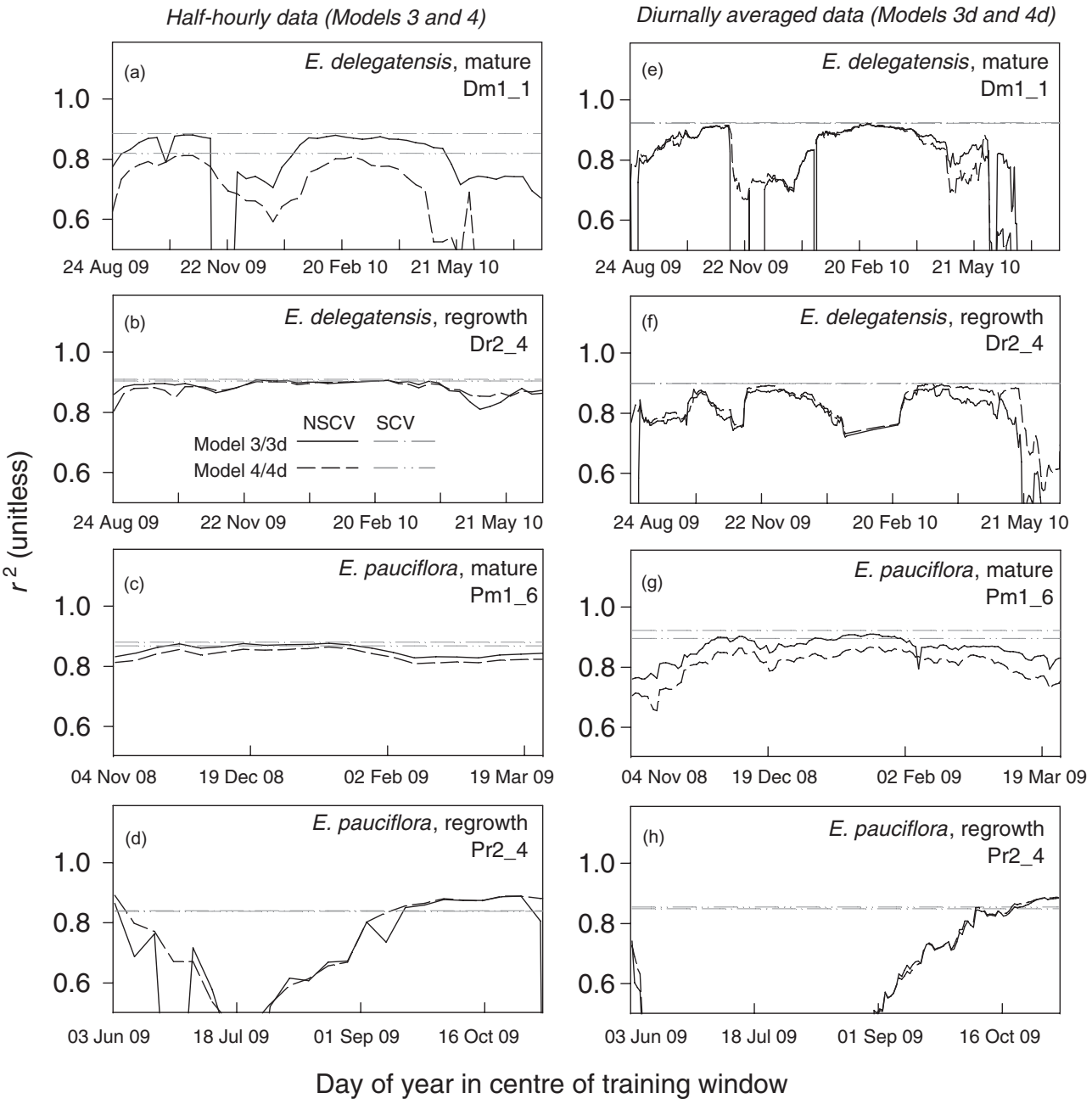

Figure 6. Coefficients of determination (r^2) for measured versus predicted sap flux from nonstationary cross-validation (NSCV) of Models 4 and 4d (solid lines) and 3 and 3d (dashed lines) for one representative tree from each species/age class group. Models were trained using a 28 d 'training window' of data centred at the date shown, and tested using the remainder of the dataset. For reference, median r^2 values from stationary cross validation (SCV), in which the training data were randomly selected from across the dataset, are shown with grey horizontal lines (dash-dot: Models 4 and 4d; dash-dot-dot: Models 3 and 3d).

In our models, the coordination of g_s with photosynthetic capacity occurs chiefly via plant hydraulic conductance, K_l, which is well known to scale with photosynthetic capacity (Brodribb & Feild 2000; Hubbard *et al.* 2001; Brodribb, Holbrook & Gutierrez 2002; Brodribb *et al.* 2005), and which affects the parameters E_m, k and b linearly. The parameter α_m is also expected to track photosynthetic capacity (as discussed in the Appendix); however, α_m appears in our models only in a ratio with K_l – in the lumped parameter b ($K_l/\chi a_m$). The tendency for both K_l and α_m to track photosynthetic capacity suggests that b should be relatively insensitive to photosynthetic capacity.

Conservation of b has already been shown, albeit indirectly. Oren *et al.* (1999) presented an empirical model for the stomatal response to evaporative demand, of the form $g_{sm} = g_{s,ref} - m \cdot \ln[D/\text{kPa}]$, where g_{sm} is g_s in saturating light, $g_{s,ref}$ is the value of g_{sm} at $D = 1$ kPa and m is the sensitivity of g_{sm} to relative changes in D. Those authors found a strong

Table 6. Best-fit parameters (mean ± SE) from stationary cross-validation of Models 3 and 4 on half-hourly data

	Model 3			Model 4			
Group	f_m	k	i_o	f_m	k	b	i_o
E. delegatensis (M)	15.3 ± 1.5	3400 ± 1600	61 ± 11	20.4 ± 2.2	496 ± 85	6.1 ± 1.4	6.6 ± 0.9
E. delegatensis (R)	26.5 ± 1.4	870 ± 230	11 ± 3	28.8 ± 1.8	680 ± 150	0.9 ± 0.3	5.9 ± 1.2
E. pauciflora (M)	15.2 ± 2.2	4940 ± 1380	123 ± 28	17.1 ± 2.4	2040 ± 440	3.5 ± 0.7	37.3 ± 7.8
E. pauciflora (R)	21 ± 1.0	3640 ± 690	38.2 ± 5.4	20.3 ± 0.9	4080 ± 840	-0.9 ± 0.3	47.7 ± 5.1

Units are: f_m, cm^3 cm^{-2} h^{-1}; k, μmol m^{-2} s^{-1} (mmol mol^{-1}); i_o, μmol m^{-2} s^{-1}; b, mmol mol^{-1}.
M, mature; R, regrowth.

Table 7. Best-fit parameters (mean ± SE) from stationary cross-validation of Models 3d and 4d on diurnally averaged data

	Model 3d		Model 4d		
Group	f_m	k	f_m	k	b
E. delegatensis (M)	12.6 ± 1.4	2180 ± 430	13.8 ± 1.8	1860 ± 430	1.4 ± 0.6
E. delegatensis (R)	13.9 ± 0.9	550 ± 100	14.0 ± 0.9	535 ± 94	*0.1 ± 0.1*
E. pauciflora (M)	12.7 ± 1.8	3640 ± 720	13.4 ± 1.8	1910 ± 390	*2.5 ± 0.7*
E. pauciflora (R)	10.6 ± 0.5	1560 ± 320	10.2 ± 0.5	1700 ± 370	*–0.8 ± 0.4*

Parameter values that were insignificant (median $P > 0.05$) in model fits are shown in italics.
Units are: f_m, cm^3 cm^{-2} h^{-1}; k, μmol m^{-2} s^{-1} (mmol mol^{-1}); b, mmol mol^{-1}.

correlation between $g_{s,ref}$ and m with a slope of 0.6, and showed this was consistent with the hypothesis that the stomatal response to D tends to keep leaf water potential, ψ_{leaf}, just above the threshold for runaway xylem cavitation (Oren *et al.* 1999). Our models allow that threshold water potential to be specified explicitly (it is $-\pi_e$ plus or minus a safety margin, as shown in the Appendix; π_e appears in the lumped parameter E_m), while also allowing the sensitivity of the D response above the threshold to vary in relation to hydraulic conductance. Additionally, our models clarify what it means for m to be proportional to $g_{s,ref}$. In the BMF model (Eqn 1), the quantity analogous to m ($-dg_{sm}/d\ln D$) equals

$$-\frac{dg_{sm}}{d\ln D} = \frac{DK_l(\psi_{soil}+\pi_e)}{(K_l/\chi\alpha_m + D)^2} = g_s(\alpha_m, D)\cdot\left(\frac{D}{K_l/\chi\alpha_m + D}\right) \quad (13)$$

where $g_s(\alpha_m,D)$ is g_{sm}, that is, g_s with α set to α_m to represent saturating light, but with D unspecified. At $D = 1$ kPa (10 mmol mol^{-1} in our units), $g_s(\alpha_m,D)$ equals $g_{s,ref}$ by definition:

$$-\left.\frac{dg_{sm}}{d\ln D}\right|_{D=1kPa} = g_{s,ref}\cdot\left(\frac{10}{K_l/\chi\alpha_m + 10}\right) \quad (14)$$

The term in parentheses is analogous to the conserved slope of 0.6 in the Oren model. Thus, our models suggest an explanation for the conservation of that slope: namely, that K_l and $\chi\alpha_m$ are adaptively coordinated across species in a ratio of approximately 20:3 ($K_l/\chi\alpha_m = 20/3$ makes the term in parentheses above equal to 0.6). Because $K_l/\chi\alpha_m$ is the parameter b in our derived models, this suggests that the body of work showing $g_{s,ref} \approx 0.6\,m$ (Oren *et al.* 1999, 2001; Ewers *et al.* 2001) can be assimilated into our derived models simply by setting $b = 20/3$. We note as well that if $b = 20/3$, then $g_{s,ref} = 0.06K_l(\psi_{soil} + \pi_e) = 0.06E_m$ (to see this,

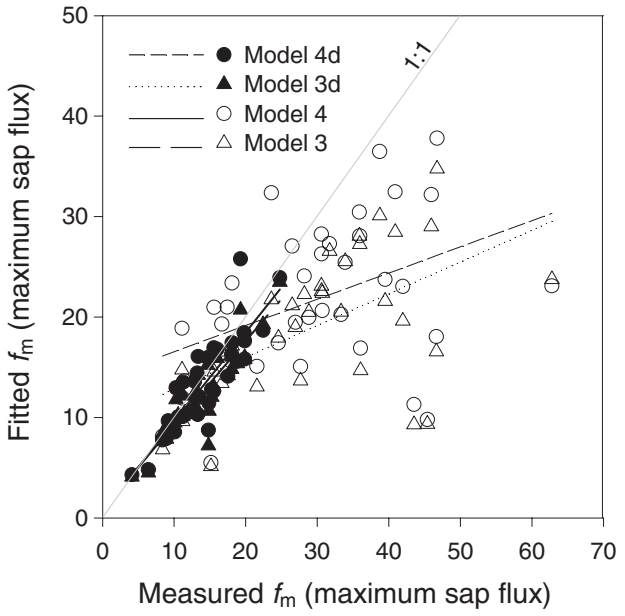

Figure 7. Measured versus fitted values of maximum sap flux, f_m, for each model. Each point represents a different tree; fitted values are medians from stationary cross-validation. Regression equations are: y = 0.89x + 0.60, $r^2 = 0.76$ (Model 4d); y = 0.83x + 0.90, $r^2 = 0.81$ (Model 3d); y = 0.26x + 13.93, $r^2 = 0.18$ (Model 4); y = 0.32x + 9.68, $r^2 = 0.31$ (Model 3).

substitute $K_l/\chi\alpha = 20/3$ and $D_s = 10$ in Eqn 1). This allows $g_{s,ref}$ to be estimated from physiological variables, or E_m to be estimated from published values of $g_{s,ref}$.

Conservation of the ratio $K_l/\chi\alpha_m$ expresses the growing understanding that hydraulic conductance is conservatively coordinated with photosynthetic capacity (which in the BMF model affects α_m) (Brodribb & Feild 2000; Hubbard *et al*. 2001; Brodribb *et al*. 2002, 2005; Katul, Leuning & Oren 2003). Our models extend those insights by providing a tool to interpret or predict deviations of $K_l/\chi\alpha_m$ from the conservative averages reported previously. For example, in the original BMF model, α_m captures the direct effect of hormonal drought signals such as abscisic acid on stomatal regulation (Buckley *et al*. 2003). This generates a testable hypothesis: exposure to drought-derived ABA signals should increase $K_l/\chi\alpha_m$ in leaves, or decrease the Oren slope ($-dg_{sm}/d\ln D$). Similarly, we would hypothesize an increase in $K_l/\chi\alpha_m$ under CO_2 enrichment in species that exhibit photosynthetic down-regulation without a corresponding decline in hydraulic conductance (e.g. Heath *et al*. 1997; Tognetti *et al*. 1998).

CONCLUSION

Simple models for stomatal conductance derived from the BMF process model of stomatal conductance (Buckley *et al*. 2003) but requiring only two to four parameters performed well in cross-validation using long sap flux datasets (176–365 d) from 36 trees of two *Eucalyptus* species and age classes in seven subalpine stands in southeastern Australia. We found that the models could be trained to near-maximal accuracy using 1 month of sap flux data from spring or autumn. A four-parameter model predicted variations in nocturnal transpiration well by assuming persistent nocturnal stimulation of guard cell osmotic pressure equivalent to that expected under ~0.5% of midday summer irradiance. We showed how experimentally derived knowledge about effects of CO_2 enrichment on biophysical parameters in the BMF model can be used to adjust parameters in the derived models, and how our models accommodate and extend insights from widely used empirical models of stomatal conductance. Our derived models can help to bridge the gap between detailed process models and purely empirical models.

ACKNOWLEDGMENTS

We thank Michael Kemp for singularly sedulous technical support in the field, and Alexandra Barlow, Chantelle Doyle, Meaghan Jenkins, Jöerg Kruse, John Larmour, Jessica O'Brien, Stephen Roxburgh, Scott Stephens, Megan Webb and Heather Vice for additional support in the field. This work was funded by the Bushfire Cooperative Research Centre (Australia) and by a Linkage Grant (LP 0989881) from the Australian Research Council and ACTEW Corporation.

REFERENCES

Ainsworth E.A. & Long S.P. (2005) What have we learned from 15 years of free-air CO_2 enrichment (FACE)? A meta-analytic review of the responses of photosynthesis, canopy properties and plant production to rising CO_2. *New Phytologist* **165,** 351–372.

Arlot S. & Celisse A. (2010) A survey of cross-validation procedures for model selection. *Statistics Surveys* **4,** 40–79.

Arndt S.K., Livesley S.J., Merchant A., Bleby T.M. & Grierson P.F. (2008) Quercitol and osmotic adaptation of field-grown Eucalyptus under seasonal drought stress. *Plant, Cell & Environment* **31,** 915–924.

Ball J.T., Woodrow I.E. & Berry J.A. (1987) A model predicting stomatal conductance and its contribution to the control of photosynthesis under different environmental conditions. In *Progress in Photosynthesis Research* (ed. J. Biggens), pp. 221–224. Martinus Nijhoff Publishers, Dordrecht, The Netherlands.

Barbour M.M. & Buckley T.N. (2007) The stomatal response to evaporative demand persists at night in *Ricinus communis* plants with high nocturnal conductance. *Plant, Cell & Environment* **30,** 711–721.

Battaglia M., Sands P., White D. & Mummery D. (2004) CABALA: a linked carbon, water and nitrogen model of forest growth for silvicultural decision support. *Forest Ecology and Management* **193,** 251–282.

Bergmeir C. & Benîtez J.M. (2012) On the use of cross-validation for time series predictor evaluation. *Information Sciences* **191,** 192–213.

Bleby T.M., Burgess S.S.O. & Adams M.A. (2004) A validation, comparison and error analysis of two heat-pulse methods for measuring sap flow in *Eucalyptus marginata* saplings. *Functional Plant Biology* **31,** 645–658.

Brodribb T.J. & Feild T.S. (2000) Stem hydraulic supply is linked to leaf photosynthetic capacity: evidence from New Caledonian and Tasmanian rainforests. *Plant, Cell & Environment* **23,** 1381–1388.

Brodribb T.J., Holbrook N.M. & Gutierrez M.V. (2002) Hydraulic and photosynthetic coordination in seasonally dry tropical forest trees. *Plant, Cell & Environment* **25,** 1435–1444.

Brodribb T.J., Holbrook N.M., Zwieniecki M.A. & Palma B. (2005) Leaf hydraulic capacity in ferns, conifers and angiosperms: impacts on photosynthetic maxima. *New Phytologist* **165,** 839–846.

Buckley T.N. (2005) The control of stomata by water balance (Tansley Review). *New Phytologist* **168,** 275–292.

Buckley T.N. & Mott K.A. (2002) Stomatal water relations and the control of hydraulic supply and demand. *Progress in Botany* **63,** 309–325.

Buckley T.N., Mott K.A. & Farquhar G.D. (2003) A hydromechanical and biochemical model of stomatal conductance. *Plant, Cell & Environment* **26,** 1767–1785.

Buckley T.N., Turnbull T.L., Pfautsch S. & Adams M.A. (2011) Nocturnal water loss in mature subalpine *Eucalyptus delegatensis* tall open forests and adjacent *E. pauciflora* woodlands. *Ecology and Evolution* **1,** 435–450.

Burgess S.S.O., Adams M.A., Turner N.C., Beverly C.R., Ong C.K., Khan A.A.H. & Bleby T.M. (2001) An improved heat pulse method to measure low and reverse rates of sap flow in woody plants. *Tree Physiology* **21,** 589–598.

Burman P. (1989) A comparative study of ordinary cross-validation, v-fold cross-validation and the repeated learning-testing methods. *Biometrika* **76,** 503–514.

Caird M.A., Richards J.H. & Donovan L.A. (2007) Nighttime stomatal conductance and transpiration in C_3 and C_4 plants. *Plant Physiology* **143,** 4–10.

Cavender-Bares J., Sack L. & Savage J. (2007) Atmospheric and soil drought reduce nocturnal conductance in live oaks. *Tree Physiology* **27,** 611–620.

Collatz G.J., Ball J.T., Grivet C. & Berry J.A. (1991) Physiological and environmental regulation of stomatal conductance, photosynthesis and transpiration: a model that includes a laminar boundary layer. *Agricultural and Forest Meteorology* **54,** 107–136.

Collins M., An S.-I., Cai W., *et al*. (2011) The impact of global warming on the tropical Pacific Ocean and El Nino. *Nature Geosci* **3,** 391–397.

Damour G., Simonneau T., Cochard H. & Urban L. (2010) An overview of models of stomatal conductance at the leaf level. *Plant, Cell & Environment* **33,** 1419–1438.

Dawson T.E., Burgess S.S.O., Tu K.P., Oliveira R.S., Santiago L.S., Fisher J.B., Simonin K.A. & Ambrose A.R. (2007) Nighttime transpiration in woody plants from contrasting ecosystems. *Tree Physiology* **27,** 561–575.

Dewar R.C. (1995) Interpretation of an empirical model for stomatal conductance in terms of guard cell function. *Plant, Cell & Environment* **18,** 365–372.

Dewar R.C. (2002) The Ball-Berry-Leuning and Tardieu-Davies stomatal models: synthesis and extension within a spatially aggregated picture of guard cell function. *Plant, Cell & Environment* **25,** 1383–1398.

Domec J.-C., Palmroth S., Ward E., Maier C.A., Thérézien M. & Oren R.A.M. (2009) Acclimation of leaf hydraulic conductance and stomatal conductance of *Pinus taeda* (loblolly pine) to long-term growth in elevated CO2 (free-air CO2 enrichment) and N-fertilization. *Plant, Cell & Environment* **32,** 1500–1512.

Ewers B.E., Oren R., Phillips N., Strömgren M. & Linder S. (2001) Mean canopy stomatal conductance responses to water and nutrient availabilities in *Picea abies* and *Pinus taeda*. *Tree Physiology* **21,** 841–850.

Farquhar G.D. & Wong S.C. (1984) An empirical model of stomatal conductance. *Australian Journal of Plant Physiology* **11,** 191–210.

Farquhar G.D., von Caemmerer S. & Berry J.A. (1980) A biochemical model of photosynthetic CO_2 assimilation in leaves of C_3 species. *Planta* **149,** 78–90.

Ford C.R., Hubbard R.M., Kloeppel B.D. & Vose J.M. (2007) A comparison of sap flux-based evapotranspiration estimates with catchment-scale water balance. *Agricultural and Forest Meteorology* **145,** 176–185.

Franks P.J. & Farquhar G.D. (2007) The mechanical diversity of stomata and its significance in gas-exchange control. *Plant Physiology* **143,** 78–87.

Gao Q., Zhao P., Zeng X., Cai X. & Shen W. (2002) A model of stomatal conductance to quantify the relationship between leaf transpiration, microclimate and soil water stress. *Plant, Cell & Environment* **25,** 1373–1381.

Granger R.J. & Pomeroy J.W. (1997) Sustainability of the western Canadian boreal forest under changing hydrological conditions – summer energy and water use. In *Sustainability of Water Resources under Increasing Uncertainty* (eds D. Rosjberg, N. Boutayeb, A. Gustard, Z. Kundzewicz & P. Rasmussen), pp. 243–250. IAHS Press, Wallingford, UK.

Heath J., Kerstiens G. & Tyree M.T. (1997) Stem hydraulic conductance of European beech (*Fagus sylvatica* L.) and pedunculate oak (*Quercus robur* L.) grown in elevated CO2. *Journal of Experimental Botany* **48,** 1487–1489.

Houborg R., Anderson M.C., Norman J.M., Wilson T. & Meyers T. (2009) Intercomparison of a 'bottom-up' and 'top-down' modeling paradigm for estimating carbon and energy fluxes over a variety of vegetative regimes across the U.S. *Agricultural and Forest Meteorology* **149,** 1875–1895.

Hubbard R.M., Ryan M.G., Stiller V. & Sperry J.S. (2001) Stomatal conductance and photosynthesis vary linearly with plant hydraulic conductance in ponderosa pine. *Plant, Cell & Environment* **24,** 113–121.

Jackson R.B., Sala O.E., Paruelo J.M. & Mooney H.A. (1998) Ecosystem water fluxes for two grasslands in elevated CO_2: a modeling analysis. *Oecologia* **113,** 537–546.

Jarvis A.J. & Davies W.J. (1998) The coupled response of stomatal conductance to photosynthesis and transpiration. *Journal of Experimental Botany* **49,** 399–406.

Jarvis P.G. (1976) The interpretation of the variations in leaf water potential and stomatal conductance found in canopies in the field. *Philosophical Transactions of the Royal Society of London, Series B* **273,** 593–610.

Katul G., Leuning R. & Oren R. (2003) Relationship between plant hydraulic and biochemical properties derived from a steady-state coupled water and carbon transport model. *Plant, Cell & Environment* **26,** 339–350.

Korol R.L., Running S.W. & Milner K.S. (1995) Incorporating intertree competition into an ecosystem model. *Canadian Journal of Forest Research* **25,** 413–424.

Leuning R. (1995) A critical appraisal of a combined stomatal-photosynthesis model for C_3 plants. *Plant, Cell & Environment* **18,** 339–357.

Leuning R., Kelliher F.M., de Pury D.G.G. & Schulze E.D. (1995) Leaf nitrogen, photosynthesis, conductance and transpiration: scaling from leaves to canopies. *Plant, Cell & Environment* **18,** 1183–1200.

Levia D.F., Carlyle-Moses D.E. & Tanaka T. (2011) Reflections on the state of forest hydrology and biogeochemistry. In *Forest Hydrology and Biogeochemistry: Synthesis of past Research and Future Directions* (eds D.F. Levia, D.E. Carlyle-Moses & T. Tanaka), p. 740. Springer, Dordrecht, the Netherlands.

Lloyd J., Wong S.C., Styles J.M., Batten D., Priddle R., Turnbull C. & McConchie C.A. (1995) Measuring and modelling whole-tree gas exchange. *Functional Plant Biology* **22,** 987–1000.

Merchant A., Arndt S., Rowell D., Posch S., Callister A., Tausz M. & Adams M. (2010) Seasonal changes in carbohydrates, cyclitols, and water relations of 3 field grown *Eucalyptus* species from contrasting taxonomy on a common site. *Annals of Forest Science* **67,** 104–104.

Morgan J.M. (1984) Osmoregulation and water stress in higher plants. *Annual Review of Plant Physiology* **35,** 299–319.

Noe S.M. & Giersch C. (2004) A simple dynamic model of photosynthesis in oak leaves: coupling leaf conductance and photosynthetic carbon fixation by a variable intracellular CO_2 pool. *Functional Plant Biology* **31,** 1195–1204.

Oren R., Sperry J.S., Katul G.G., Pataki D.E., Ewers B.E., Phillips N. & Schafer K.V.R. (1999) Survey and synthesis of intra- and interspecific variation in stomatal sensitivity to vapour pressure deficit. *Plant, Cell & Environment* **22,** 1515–1526.

Oren R., Sperry J.S., Ewers B.E., Pataki D.E., Phillips N. & Megonigal J.P. (2001) Sensitivity of mean canopy stomatal conductance to vapor pressure deficit in a flooded *Taxodium distichum* L. forest: hydraulic and non-hydraulic effects. *Oecologia* **126,** 21–29.

Paruelo J.M. & Sala O.E. (1995) Water losses in the patagonian steppe: a modelling approach. *Ecology* **76,** 510–520.

Peak D. & Mott K.A. (2011) A new, vapour-phase mechanism for stomatal responses to humidity and temperature. *Plant, Cell & Environment* **34,** 162–178.

Phillips N.G., Lewis J.D., Logan B.A. & Tissue D.T. (2010) Inter- and intra-specific variation in nocturnal water transport in *Eucalyptus*. *Tree Physiology* **30,** 586–596.

Pomeroy J.W., Gray D.M., Brown T., Hedstrom N.R., Quinton W.L., Granger R.J. & Carey S.K. (2007) The cold regions hydrological

model: a platform for basing process representation and model structure on physical evidence. *Hydrological Processes* **21,** 2650–2667.

de Pury D.G.G. & Farquhar G.D. (1997) Simple scaling of photosynthesis from leaves to canopies without the errors of big-leaf models. *Plant, Cell & Environment* **20,** 537–557.

Raupach M.R. & Finnigan J.J. (1988) ';Single-layer models of evaporation from plant canopies are incorrect but useful, whereas multilayer models are correct but useless': discuss. *Functional Plant Biology* **15,** 705–716.

Rauscher H.M., Isebrands J.G., Host G.E., Dickson R.E., Dickmann D.I., Crow T.R. & Michael D.A. (1990) ECOPHYS: an ecophysiological growth process model for juvenile poplar. *Tree Physiology* **7,** 255–281.

Reichstein M., Tenhunen J.D., Roupsard O., Ourcival J., Rambal S., Miglietta F., Peressotti A., Pecchiari M., Tirone G. & Valentini R. (2002) Severe drought effects on ecosystem CO2 and H2O fluxes at three Mediterranean evergreen sites: revision of current hypotheses? *Global Change Biology* **8,** 999–1017.

Running S.W. & Coughlan J.C. (1988) A general model of forest ecosystem processes for regional applications 1. Hydrologic balance, canopy gas exchange and primary production processes. *Ecological Modelling* **42,** 125–154.

Staudte R.G. & Sheather S.J. (1990) *Robust Estimation and Testing*. John Wiley and Sons, New York, USA.

Tognetti R., Longobucco A., Miglietta F. & Raschi A. (1998) Transpiration and stomatal behaviour of *Quercus ilex* plants during the summer in a Mediterranean carbon dioxide spring. *Plant, Cell & Environment* **21,** 613–622.

Van Wijk M.T., Dekker S.C., Bouten W., Bosveld F.C., Kohsiek W., Kramer K. & Mohren G.M.J. (2000) Modeling daily gas exchange of a Douglas-fir forest: comparison of three stomatal conductance models with and without a soil water stress function. *Tree Physiology* **20,** 115–122.

White D.A., Beadle C.L., Sands P.J., Worledge D. & Honeysett J.L. (1999) Quantifying the effect of cumulative water stress on stomatal conductance of *Eucalyptus globulus* and *Eucalyptus nitens*: a phenomenological approach. *Functional Plant Biology* **26,** 17–27.

Wilson K.B., Hanson P.J., Mulholland P.J., Baldocchi D.D. & Wullschleger S.D. (2001) A comparison of methods for determining forest evapotranspiration and its components: sap-flow, soil water budget, eddy covariance and catchment water balance. *Agricultural and Forest Meteorology* **106,** 153–168.

Wong S.C. (1979) *Stomatal Behaviour in Relation to Photosynthesis*. Australian National University, Canberra.

Zeppel M., Tissue D.T., Taylor D., Macinnis-Ng C. & Eamus D. (2010) Rates of nocturnal transpiration in two evergreen temperate woodland species with different water-use strategies. *Tree Physiology* **30,** 988–1000.

Received 16 January 2012; accepted for publication 2 April 2012

APPENDIX

Modifying lumped parameters to reflect experimental knowledge of climate change effects

In this Appendix, we demonstrate how our models can accommodate advances in physiological understanding by applying results from CO_2 enrichment experiments to the models' parameters. α_m and ϕ, which affect guard cell advantage (α, Eqn 2), can be related to parameters in the model for α used by Buckley *et al*. (2003): $\alpha = \beta\tau - M$, where β (m^2 $mmol^{-1}$) is the sensitivity of the guard-to-epidermal cell osmotic gradient to epidermal turgor, τ is [ATP] in photosynthesising cells (mmol m^{-2}) and M is the net epidermal mechanical advantage (unitless). It is easily shown from eqns A19-A22 in Buckley *et al*. (2003) that α_m, the limit of α at large irradiance, is

$$\alpha_m = \beta\left(a_t - 4p\left(\frac{V_m}{J_m}\right)\left(\frac{c_i + 2\Gamma_*}{c_i + K'}\right)\right) - M, \quad \text{(A1)}$$

where a_t and p are the total adenylate pool and concentration of photophosphorylation sites, respectively (mmol m^{-2}); V_m and J_m are carboxylation and electron transport capacity, respectively (μmol m^{-2} s^{-1}); c_i, Γ* and K' are intercellular CO_2 concentration, photorespiratory CO_2 compensation point and effective Michaelis constant for RuBP carboxylation, respectively (μmol mol^{-1}). A meta-analysis of free-air CO_2 enrichment (FACE) experiments by Ainsworth & Long (2005) found that V_m declined on average by 6%, J_m by 1% and V_m/J_m by 5% across tree species following a ~200 μmol mol^{-1} increase in CO_2 (c_a). If a_t and p scale with V_m as suggested by Farquhar & Wong (1984), then they too are expected to decline by 6%. We can then estimate the ratio of α_m at elevated CO_2 (580 μmol mol^{-1}) to ambient CO_2 (380 μmol mol^{-1}), using typical values of the parameters in A1 (a_t, 6.3; p, 1.3 (Farquhar & Wong 1984); Γ*, 37; K', 738; V_m/J_m, 0.48 (de Pury & Farquhar 1997); c_i, 0.7 c_a (Ainsworth & Long 2005); β, 1.17; M, 1 (Buckley *et al*. 2003), using square brackets to indicate terms affected by CO_2 enrichment:

$$\frac{\alpha_m'}{\alpha_m} = \frac{1.17\left([0.94\cdot 6.3] - 4[0.94\cdot 1.3][0.95\cdot 0.48]\left(\frac{0.7\cdot[580]+2\cdot 37}{0.7\cdot[580]+738}\right)\right) - 1}{1.17\left(6.3 - 4\cdot 1.3\cdot 0.48\left(\frac{0.7\cdot 380+2\cdot 37}{0.7\cdot 380+738}\right)\right) - 1} = 0.90, \quad \text{(A2)}$$

α_m should thus decrease by about 10%, barring any change in β or M. Using a conserved c_i/c_a ratio implicitly captures the direct stomatal response to CO_2, which preserves that ratio (Wong 1979; Ball *et al*. 1987).

An expression for ϕ, the initial slope of the response of α to light, is found by applying the chain rule to Eqns A20, A21 and A23 in Buckley *et al*. (2003) to give:

$$\phi = \frac{\phi'\beta}{4}\left(\frac{a_t - p}{V_m}\right)\left(1 - \frac{V_r}{V_m}\right)\left(\frac{c_i + K'}{c_i + 2\Gamma_*}\right), \quad \text{(A3)}$$

where ϕ' is the initial slope of the response of potential electron transport rate to light (e^- per hν) and V_r is the CO_2- and Rubisco-saturated but RuBP-limited carboxylation rate (μmol m^{-2} s^{-1}). Farquhar & Wong (1984) suggested a_t, p and V_r scale with V_m, implying that the first two parenthetical quantities in A3 should not change. There is no evidence that ϕ' is affected by CO_2 enrichment. The last term is the

inverse of that containing c_i in Eqn A1, so it should decrease by 19%. Thus, ϕ is expected to decline by about 19%, assuming constant β.

We may combine these predicted changes in α_m and ϕ to estimate the change in α at intermediate light, say $\phi i = \alpha_m$, from Eqn 2:

$$\frac{\alpha'}{\alpha} = \frac{0.9\alpha_m 0.81\phi i}{0.9\alpha_m + 0.81\phi i} \cdot \frac{\alpha_m + \phi i}{\alpha_m \phi i} = \frac{0.9 \cdot 0.81}{0.9\alpha_m + 0.81 \cdot \alpha_m} \cdot \frac{\alpha_m + \alpha_m}{1} = 0.85. \quad \text{(A4)}$$

Thus, α is predicted to decline by approximately 15% with CO_2 enrichment.

Threshold leaf water potential

Steady-state transpiration rate E is equal to $K_l(\psi_{soil} - \psi_{leaf})$, where ψ_{leaf} is leaf water potential. The minimum ψ_{leaf} at large D is therefore given by $\psi_{soil} - E_m/K_l$, where E_m is the limit of E at large D. Applying $E = g_s D$ to the BMF model for g_s (Eqn 1) and taking the limit at large D using L'Hôpital's Rule gives:

$$E_m = \lim_{D\to\infty} E = \lim_{D\to\infty} g_s D = \lim_{D\to\infty} \frac{K_l(\psi_{soil} + \pi_e)D}{K_l/\chi\alpha + D} = K_l(\psi_{soil} + \pi_e). \quad \text{(A5)}$$

Thus, the minimum ψ_{leaf} equals $-\pi_e$; that is, the BMF model predicts that stomata keep leaf water potential just above $-\pi_e$. If, as hypothesized by Oren et al. (1999), stomatal behaviour also keeps leaf water potential just above the critical threshold causing runaway xylem cavitation (ψ_{crit}), then ψ_{crit} must be close to $-\pi_e$. Species that exhibit a 'safety margin' (i.e. minimum ψ_{leaf} is significantly above ψ_{crit}) would have $\pi_e < \psi_{crit}$, and those with a tendency to exceed the threshold (a negative safety margin, as it were) would have $\pi_e > \psi_{crit}$.